

Initial Implementation of Transient VERA-CS

Aaron Wysocki, ORNL

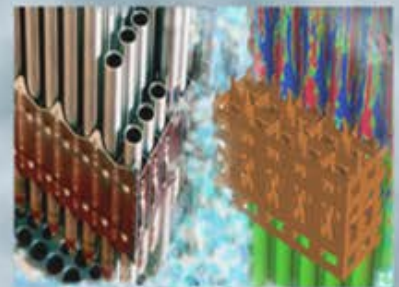
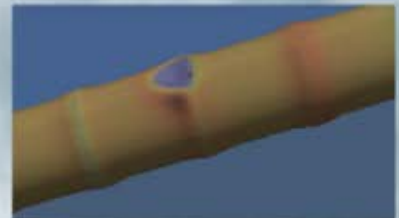
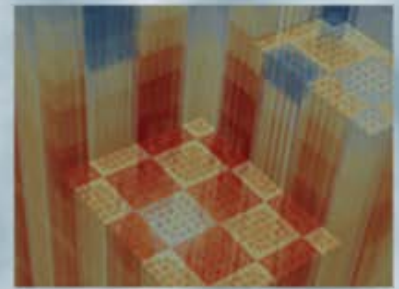
Andrew Gerlach, University of Michigan

Brendan Kochunas, University of Michigan

Robert Salko, ORNL

4/3/2017

Approved for Public Release





REVISION LOG

Revision	Date	Affected Pages	Revision Description
0	4/3/2017	All	Initial version

Document pages that are:

Unlimited All

Export Controlled None

IP/Proprietary/NDA Controlled None

Sensitive Controlled None

This report was prepared as an account of work sponsored by an agency of the United States Government. Neither the United States Government nor any agency thereof, nor any of their employees, makes any warranty, express or implied, or assumes any legal liability or responsibility for the accuracy, completeness, or usefulness of any information, apparatus, product, or process disclosed, or represents that its use would not infringe privately owned rights. Reference herein to any specific commercial product, process, or service by trade name, trademark, manufacturer, or otherwise, does not necessarily constitute or imply its endorsement, recommendation, or favoring by the United States Government or any agency thereof. The views and opinions of authors expressed herein do not necessarily state or reflect those of the United States Government or any agency thereof.

Requested Distribution:

To:

Copy:

EXECUTIVE SUMMARY

In this milestone the capabilities of both CTF and MPACT were extended to perform coupled transient calculations. This required several small changes in MPACT to setup the problems correctly, perform the edits correctly, and call the appropriate CTF interfaces in the right order. For CTF, revisions and corrections to the transient timestepping algorithm were made, as well as the addition of a new interface subroutine to allow MPACT to drive CTF at each timestep.

With the modifications completed, the initial coupled capability was demonstrated on some problems used for code verification, a hypothetical small mini-core, and a Watts Bar demonstration problem. For each of these cases the results showed good agreement with the previous MPACT internal TH feedback model that relied on a simplified fuel heat conduction model and simplified coolant treatment. After the pulse the results are notably different as expected, where the effects of convection of heat to the coolant can be observed.

Areas for future work were discussed, including assessment and development of the CTF dynamic fuel deformation and gap conductance models, addition of suitable transient boiling and CHF models for the rapid heating and cooling rates seen in RIAs, additional validation and demonstration work, and areas for improvement to the code input and output capabilities.

CONTENTS

REVISION LOG	ii
EXECUTIVE SUMMARY.....	iii
FIGURES	v
ACRONYMS	vi
1 Introduction	1
2 Theory.....	1
2.1 STEADY-STATE COUPLING.....	1
2.2 TRANSIENT COUPLING	3
3 Description of Code Changes	5
3.1 MPACT development	5
3.2 CTF Coding Changes.....	6
3.2.1 CTF Modifications for Coupled Transients.....	6
3.3 User Interface.....	7
3.3.1 Existing VERA input for transient.....	7
3.3.2 Proposed VERA input for transient.....	8
3.3.3 Work performed to improve output	10
4 Results.....	12
4.1 Verification.....	12
4.1.1 CTF Verification	12
4.1.2 MPACT Verification	13
4.2 Demonstration Problems.....	18
4.2.1 Hypothetical MINI-CORE Reactor	18
4.2.2 Watts Bar.....	21
5 Conclusions and Future Work.....	25
5.1 methods improvements	25
5.2 Code output improvements	26
5.3 Additional Validation and demonstration activities.....	26
6 References	27

FIGURES

Figure 1. Illustration of Direct Coupling used with MPACT and CTF in VERA-CS.	2
Figure 2. Simplified flow chart of transient coupling scheme.....	3
Figure 3. Transient coupling scheme details with MPACT time step indices in blue and CTF time step indices in red.	4
Figure 4. MPACT Modifications for CTF Transient.....	5
Figure 5. Example of existing VERA input for RIA	7
Figure 6. Example of null transient for proposed input	8
Figure 7. Example of REA transient for proposed input	9
Figure 8. Example of Loss of flow transient.....	9
Figure 9. Example of REA transient with subsequent SCRAM and variable time	10
Figure 10. “4-mini” Transient Test Problem	14
Figure 11. Results for transient 4-mini 3D regression test with simplified T/H.....	15
Figure 12. Results for transient 4-mini 3D with CTF.....	16
Figure 13. Total core power evolution for 4-mini transient.....	17
Figure 14. Core-averaged fuel temperature and difference for 4-mini transient.	18
Figure 15. Hypothetical Mini-Core Loading Pattern and Control Rod Map.....	19
Figure 16. Neutronic results for Mini-Core REA accident with SCRAM.....	20
Figure 17. TH results for Mini-Core REA accident with SCRAM	21
Figure 18. Watts Bar HZP 0.25\$ ejection case, $t=0.005$ s.....	22
Figure 19. Watts Bar HZP 0.25\$ ejection case, $t=0.04$ s.....	22
Figure 20. Watts Bar HZP 0.25\$ ejection case, $t=0.05$ s.....	23
Figure 21. Watts Bar HZP 0.25\$ ejection case, $t=0.08$ s.....	23
Figure 22. Watts Bar HZP 0.25\$ ejection case: power and reactivity versus time	24

ACRONYMS

BWR	boiling water reactor
CASL	Consortium for Advanced Simulation of Light Water Reactors
CHF	Critical Heat Flux
CP	Challenge Problem
CPR	critical power ratio
CTF	Modernized and improved version of the COBRA-TF subchannel thermal-hydraulics code
DNBR	departure from nucleate boiling ratio
DOE	US Department of Energy
HFP	Hot Full Power
HZP	Hot Zero Power
LWR	light water reactor
MOC	method of characteristics
MPACT	Michigan parallel characteristics transport code
NRC	Nuclear Regulatory Commission
ORNL	Oak Ridge National Laboratory
RIA	reactivity insertion accident
T/H	thermal-hydraulics
UM	University of Michigan
VERA	Virtual Environment for Reactor Applications

1 INTRODUCTION

Reactivity-initiated accidents (RIAs) -- including control rod ejection (CRE) events for PWRs and control rod drop accidents (CRDAs) for BWRs -- are Condition IV events (limiting faults, i.e. postulated but not expected to occur during the lifetime of a plant) involving a rapid reactivity insertion, potentially in excess of 1\$. This results in a severe power excursion which has the potential to violate General Design Criterion 28 (GDC28) of 10CFR50 Appendix A, which requires assurance that postulated reactivity accidents will neither:

- result in damage to the reactor coolant pressure boundary greater than limited local yielding, nor
- sufficiently impair core cooling capability.

Historically, the acceptance criteria for satisfying GDC28 was a maximum allowable fuel radial average energy density of 280 cal/g. However, in 2007, the NRC issued more limiting, interim RIA acceptance criteria [1]: 150-170 cal/g at zero power conditions, a provision that DNBR and CPR limits must not be exceeded at intermediate and full power conditions, and additional corrosion-dependent fuel enthalpy limits. The first two are intended to protect against high cladding temperature failure, while the third criterion is intended to protect against PCMI failure. Additional criteria on fuel enthalpy, peak fuel temperature, and rod burst/fragmentation were imposed to ensure core coolability.

In 2016, the NRC issued draft regulatory guide DG-1327 [2], which provides updated guidance for analyzing RIA events and defines fuel cladding failure thresholds for ductile failure, brittle failure, and PCMI, as well as providing radionuclide release fractions for assessing radiological consequences.

The 2007 letter, and particularly DG-1327 (if accepted), will have created a much more restrictive regulatory environment with respect to RIA events relative to the legacy rules. Additionally, these recent developments require a substantial increase in the complexity and level of physical fidelity required to demonstrate regulatory compliance. By including RIA in the list of Challenge Problems, CASL has identified RIA as an area which is both important to the nuclear industry and amenable to modern modeling and simulation techniques.

The goal of the current milestone is to perform an initial implementation of a transient VERA-CS capability to lay the groundwork for RIA-type simulations for PWRs. The results shown in this report are preliminary, and a discussion on planned improvements is given in the Future Work section at the end of the document.

2 THEORY

2.1 STEADY-STATE COUPLING

This Milestone demonstrates that the MPACT and CTF coupling has been extended to cover transients. The two codes were previously coupled for steady-state application, with MPACT acting as the 'master' code. In this configuration, MPACT calculates a converged neutronic solution and passes the local power densities to CTF. Using this power density distribution, CTF calculates the steady-state thermal-hydraulic (T/H) solution and passes the fuel temperatures, clad temperatures, moderator temperatures, and moderator densities back to MPACT, where the material cross-sections are updated accordingly. The

calculation proceeds iteratively in this manner until the eigenvalue and flux are sufficiently converged [3].

Within MPACT and CTF, the spatial discretizations are different as a result of their numerical methods, and the mapping of information (e.g., power, temperature, density) between the mesh in each code was designed to preserve the respective temperature/fluid and nuclide/neutron fields. The mesh for the coupling or solution transfer between CTF and MPACT is based on the x-y Cartesian grid formed by the pin cell geometry and the axial mesh defined by the user. An example of the pin cell geometry in x-y is illustrated in Figure 1. For each mesh (e.g., pin cell) in this grid, the solution variables in each code are integrated over the axial segment and transferred. Thus quantities like power and mass are conserved between the codes for each axial pin cell region when transferring solution data between the codes.

The pin cell averaged coupling for a 2×2 array of pin cells is illustrated in Figure 1 which shows on the left an illustration of the spatial mesh used in MPACT for the 2-D MOC calculation. Each region bounded by black lines represents a discrete spatial cell in which a unique power density may be calculated. On the right of Figure 1 is the subchannel mesh; again the black lines indicate the boundaries of discrete spatial cells within which the solution for the temperature or density has a discrete value. Figure 1 does not show the mesh used for the conduction solve in CTF which is performed over the dark gray regions in the figure representing the solid regions in the subchannel mesh. In Figure 1 the symbol T refers to the temperature, ρ is the density, and q'' is the volumetric heat generation rate. The over-bar notation indicates that the quantity has been averaged over a material region within the pin cell, and the subscript indicates the material region.

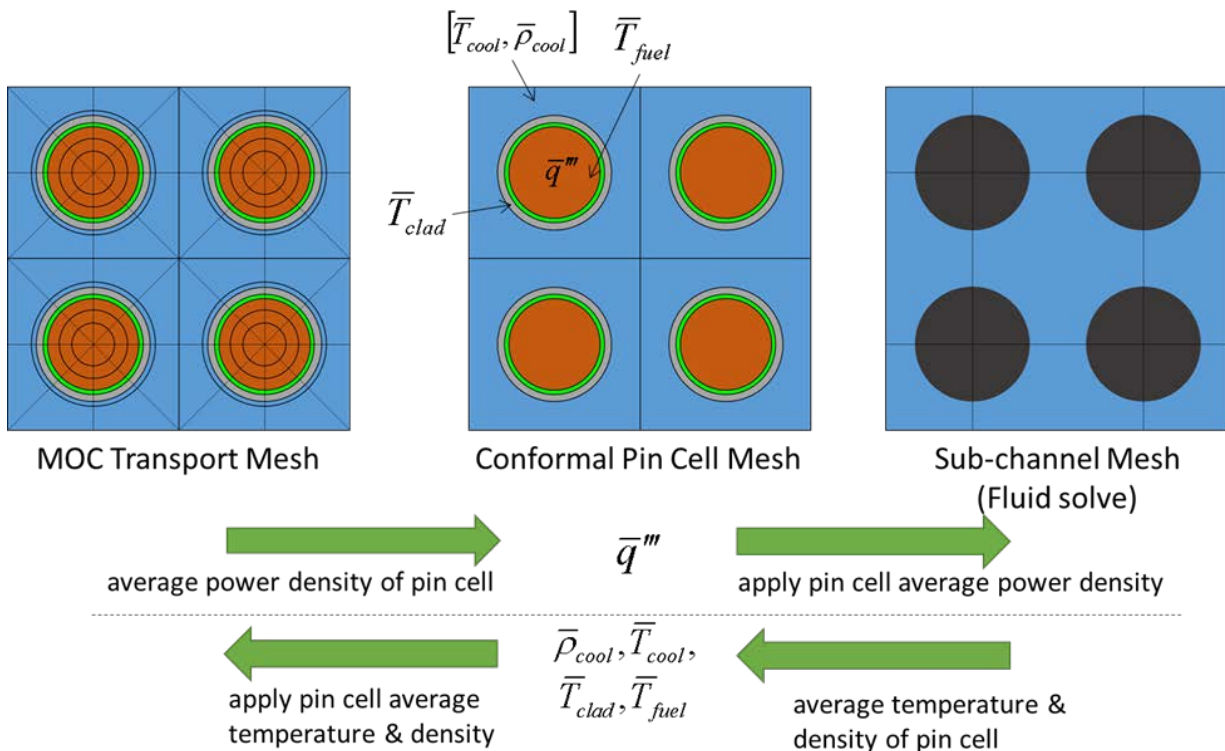


Figure 1. Illustration of Direct Coupling used with MPACT and CTF in VERA-CS.

2.2 TRANSIENT COUPLING

In the steady-state configuration, an iteration is performed between independent MPACT and CTF solutions. For transient applications, additional framework was required to pass time information between the two codes. At each time step, MPACT calls upon CTF to run a transient between the beginning and end of the time step.

For the coupled transient calculation, the same basic sequence as the coupled steady-state calculation is followed. However, no iteration is performed between the two codes during the transient. A standard coupled steady-state calculation, as described in Section 2.1, is performed to determine the initial power distribution and T/H conditions at time $t = 0$. Using the initial T/H conditions, MPACT performs a neutronic solve for the end of the first time step. The resulting power distribution is passed to CTF and used to calculate the T/H conditions at the end of the time step. The calculation proceeds thusly with MPACT performing each neutronic solve with the T/H conditions from the *beginning* of the time step and CTF performing each T/H solve with the power distribution from the *end* of the time step. This scheme is depicted in Figure 2.

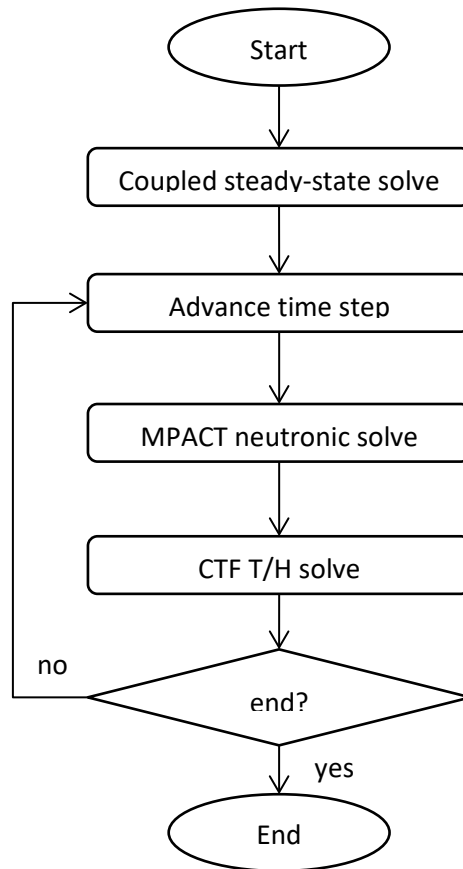


Figure 2. Simplified flow chart of transient coupling scheme.

Of note, MPACT currently advances through the transient with uniform time steps. CTF utilizes adaptive time-steps that are typically smaller than the MPACT time step. This means that for each MPACT time step, CTF effectively runs a mini-transient from the

3 DESCRIPTION OF CODE CHANGES

To develop the initial capability to perform transients with VERA-CS (e.g. MPACT coupled to CTF), modifications were needed in both MPACT and CTF.

3.1 MPACT DEVELOPMENT

The majority of the work for the transient capability in MPACT was completed in the DOE reportable milestone, L2:RTM.P13.03, from the previous PoR. To extend this capability, which used the simplified internal T/H to perform transient conduction but no convection, the coupling capabilities added for the internal solver need to be extended to the CTF interface.

Because of the object-oriented design of MPACT these changes required marginal effort. Effectively, this required only the changes shown in Figure 4.

<pre> SUBROUTINE solve_CTF(this) CLASS(CTF_CouplerType), INTENT(IN) & :: this IF(this%ctf_proc) & CALL CTF_Solve_Standalone() ENDSUBROUTINE </pre>	<pre> SUBROUTINE solve_CTF(this,dttime) CLASS(CTF_CouplerType), INTENT(IN) & :: this REAL(SRK), OPTIONAL, INTENT(IN) & :: dttime IF(this%ctf_proc) THEN IF(PRESENT(dttime)) THEN CALL CTF_Solve_Transient(dttime) ELSE CALL CTF_Solve_Standalone() ENDIF ENDIF ENDSUBROUTINE </pre>
--	---

Figure 4. MPACT Modifications for CTF Transient

However, there were numerous ancillary changes to MPACT that did require a little more effort. Briefly these changes were:

- modifications to the logic for calling feedback routines
- modifications to the MPACT driver to setup the appropriate objects and coupling interfaces for transient
- modifications to the parallel communication of the T/H data in MPACT
- modifications to the edit capabilities in MPACT for transient
- enabling the exponential transformation of the amplitude function in TML
- modifications to allow for a reactor scram following a rod eject
- modifications so that MPACT calls the CTF edits appropriately for transient

3.2 CTF CODING CHANGES

The CTF code modifications for this milestone consist of changes to the standalone CTF transient functionality (namely, the forcing functions), as well as modifications to support coupled transient calculations driven by MPACT.

3.2.1 CTF MODIFICATIONS FOR COUPLED TRANSIENTS

Considerable modifications and improvements were required internally in CTF to perform proper timestepping during coupled MPACT-CTF transients. A new subroutine, 'CTF_Solve_Transient', was added to the CTF Coupling Interface; this subroutine, modeled in part after 'CTF_Solve_Standalone', is called by MPACT for each MPACT MOC iteration step. After each call to 'CTF_Solve_Transient', MPACT then calls the appropriate 'getter' subroutines (e.g. 'CTF_get_coolant_dens') to obtain the updated TH solution values at each axial node of each fuel pin in the model.

There are two types of timesteps in a VERA-CS transient: the coupled timestep (also known as the MPACT timestep) and the CTF internal timestep (or simply, the CTF timestep). The CTF_Solve_Transient procedure takes the coupled timestep size as input and increments the transient time in CTF by that amount. The CTF timestep size may be limited by several factors, such as the Courant-Friedrichs-Lewy (CFL) condition or a condition that reduces the timestep size if the change in solution variables is too large. This latter condition only applies to changes in the fluid solution, as the 1D radial conduction solution for the fuel is fully implicit thus a timestep size restriction for change in fuel conditions is not needed.

These conditions typically make the maximum allowable CTF timestep size smaller than typical timestep sizes used by MPACT. This means that CTF will typically perform several sub-timesteps within each coarse timestep performed by MPACT. If the coupled timestep size is smaller than the CTF timestep size, the CTF timestep size will be reduced such that the CTF transient time is moved forward to the coupled transient time. There were a few issues with the internal CTF timestepping logic that needed to be addressed prior to implementing the CTF_Solve_Transient procedure.

One issue was that CTF was not ending precisely at the required transient end time; rather, it was ending the transient at the nearest time past the requested end of the transient. This normally makes little difference in standalone transients, but will lead to significant transient drift in coupled cases. CTF was fixed to reduce its final timestep size to match the exact end time of the current time interval.

An additional defect was discovered, which caused improper timestepping when the MPACT-requested time interval was less than the timestep size set by the CTF timestepping algorithm. This defect was fixed, and now CTF reduces its timestep size properly to match the MPACT-requested time interval in this scenario.

A final issue was found, wherein the CTF timestep size was being reset to the minimum allowable value each time the boundary condition 'setter' functions (e.g., 'CTF_set_inlet_flowrate') were called. The intent of this was to avoid numerical stability issues associated with sudden changes in boundary conditions. However, currently MPACT calls these before each call to 'CTF_Solve_Transient', regardless of whether the boundary condition values actually changed relative to the previous MPACT timestep. This resulted in unnecessarily high numbers of CTF iterations because the CTF timestep size had to be gradually increased from the minimum value to more reasonable values, even when the boundary conditions did not change (as is the case for most calls to

'CTF_Solve_Transient'). This issue was fixed by checking if the boundary condition actually changes when one of the 'setters' is called. If the boundary condition is not changed, the timestep size is not reduced to the minimum value.

Prior to actually coupling to MPACT and performing coupled testing, it was necessary to develop a standalone test harness for coupled transients in CTF. The CTF multistate driver was extended to test the coupled transient capability. A 'runTransient' subroutine in the multistate driver was added, which mimics the way MPACT would set the time intervals, call the TH boundary condition 'setter' functions, and call 'CTF_Solve_Transient' to drive a transient calculation. A new set of input options were added to the multistate driver allowing the user to drive a transient in CTF through the external interface.

The work described in this subsection was performed under PHI Kanban Tickets #4628, #4640, and #4748.

3.3 USER INTERFACE

The user interface consists of the input and output and post processing. Minimal work was done on the user interface to the input while some work was done for the output and post-processing. Additionally, a plan for improved VERA input was developed as a part of this milestone. In the remainder of this section we summarize the existing user input for the interface and the current plan for the new input. Then the work completed for the output and post-processing is discussed.

3.3.1 EXISTING VERA INPUT FOR TRANSIENT

The original transient capability in MPACT was implemented using the standard MPACT input and not the VERAInput. During PoR 13, work was done to port the existing options from the standard input to the VERAInput, which among other things, enabled the definition of a rod eject. To convert a normal steady-state VERA input to specify an RIA two changes were required. The first was to the [MPACT] block. This is illustrated in Figure 5. Note that some of these cards are extraneous and should be eliminated.

```
[MPACT]
prompt      true !extraneous, does not work if not set to true
accel       true !extraneous, does not work if not set to true
transmethod theta 1.0 !other options exist, but are not as robus
timestep    0.005 0.0001 0.3 !first value is fixed time step in MPACT
                                !second value is ignored
                                !third value is end time of transient

!specifies control rod is moving from 0.0 to 0.1 s, last 3 values ignored
!then nothing in system changes from 0.1 to 0.3 s, last 4 values ignored
perturb     0.0 0.1 mvcr 1 1 2
            0.1 0.3 const 1 1 2
```

Figure 5. Example of existing VERA input for RIA

The second change required defining a [STATE] block with the position of the control rod for every time step in the transient where the rod is moving. This latter requirement could become quite onerous if small time steps are used (e.g. it is conceivable that 200 lines would be required to define this motion).

Given this second requirement, and the fact that it is limited to rod ejection, the development of a more flexible and simplified user input is necessary. This is described in section 3.3.2.

3.3.2 PROPOSED VERA INPUT FOR TRANSIENT

The proposed input changes for transient are still being finalized. The stated objectives for the new input are the following:

1. Allow for processing of more input cards in [STATE] block e.g. pressure, flow, boron, tinlet, etc. to be able to specify a wider variety of transients.
2. Assume state variables change linearly between values defined at specific times
3. Allow for defining a rod eject with $O(1)$ [STATE] blocks
4. Allow for user to be able to control time step sizes for different periods in the transient or specify dynamic time stepping (after this feature is implemented).

Given these requirements we illustrate the new input in Figure 6 through Figure 9. Some discussion is still ongoing about how to handle item 4, but for the examples given the other three requirements are met. Item 3 refers to the fact that the current implementation requires a [STATE] block for each timestep during the portion of the transient where control rod movement or changes in TH boundary conditions are occurring; in other words, this requires $O(N)$ [STATE] blocks, where N is the number of timesteps (inversely proportional to timestep size). In the proposed input illustrated in the figures, control rod positions or TH boundary conditions would only need to be defined at a limited set of time points (i.e. [STATE] blocks), and MPACT would determine control rod positions and TH boundary conditions at intermediate time points by linearly interpolating the values provided in the input. In this case, the number of required [STATE] blocks would be independent of the choice of timestep size, i.e. the number of required [STATE] blocks is $O(1)$.

Additionally, for the [MPACT] block, only the time stepping method would need to be defined.

```
[STATE]
power 100.0
feedback on
sym qtr
transient_time 0.0
rod_bank A 0
          B 0
          C 0

[STATE]
transient_dt constant 0.005 !constant 5 ms time steps
transient_time 3.0          !Simulate to 3.0 seconds
```

Figure 6. Example of null transient for proposed input

```

STATE]
  power 100.0
  feedback on
  sym qtr
  transient_time 0.0
  bank_pos A 0
           B 0
           C 0
[STATE]
  transient_dt constant 0.002
  transient_time 0.08
  bank_pos A 0
           B 0
           C 200
[STATE]
  transient_time 3.0
    
```

Figure 7. Example of REA transient for proposed input

```

[STATE]
  power 100.0
  flow 100.0
  feedback on
  sym qtr
  transient_time 0.0
  bank_pos A 200
           B 200
           C 0
[STATE]
  transient_dt constant 0.01
  transient_time 0.5
  flow 80.0
[STATE]
  transient_time 1.0
  flow 50.0
[STATE]
  transient_time 2.0
  flow 10.0
[STATE]
  transient_time 3.0
  flow 9.0
    
```

Figure 8. Example of Loss of flow transient

```

[STATE]
  power 100.0
  feedback on
  sym qtr
  transient_time 0.0
  bank_pos A 200
           B 200
           C 0

[STATE]
  transient_dt constant 0.005
  transient_time 0.02

[STATE]
  transient_dt constant 0.002
  transient_time 0.08
  bank_pos A 200
           B 200
           C 200

[STATE]
  transient_dt constant 0.002
  transient_time 0.1

[STATE]
  transient_dt constant 0.005
  transient_time 1.5

[STATE]
  transient_dt constant 0.002
  transient_time 1.58
  bank_pos A 0
           B 0
           C 200

[STATE]
  transient_dt constant 0.002
  transient_time 1.6

[STATE]
  transient_dt constant 0.005
  transient_time 1.8

[STATE]
  transient_dt constant 0.01
  transient_time 3.0

```

Figure 9. Example of REA transient with subsequent SCRAM and variable time

3.3.3 WORK PERFORMED TO IMPROVE OUTPUT

Several small tasks were completed to facilitate edits during a transient calculation that mimic those of a steady-state calculation. Briefly this work involved:

- Adding the delayed neutron fraction, beta, to the HDF5 output
- Adding the transient time to the HDF5 output
- Adding the total reactivity to the HDF5 output
- Enabling edits for the T/H data in MPACT to the HDF5 output
- Enabling the edit of the current state condition to the HDF5 output file
- Adding the total power (in Watts) of the reactor to the HDF5 output file
- Adding the neutron generation time to the HDF5 output file

- Enabling the edit of core power level as percent rated power to the HDF5 output
- Enabling the edits produced by CTF for each time step to the HDF5 output

Once these edits were produced to the HDF5 output file, much of it was readily viewable in VERAView. This output is illustrated, for example, in Figure 18 through Figure 21.

Some additional quantities of interest still need to be calculated and edited. These quantities include energy deposition and component reactivity edits. Some work is also suggested for VERAView to allow viewing of the state variables, such as rod position, for transient calculations. Another item for VERAView might be adding transient time to the default set of time variables.

4 RESULTS

This section describes the results generated for this milestone. This includes some verification results used for developing regression tests and results for some demonstration problems.

4.1 VERIFICATION

Verification of the capabilities in VERA-CS typically involves the addition of a regression test, where the input for a small problem is developed and the solution is compared to a reference solution that is known to be correct. Moreover, depending on the feature, a unit test may be more suitable to verify the feature or capability. In this case, two regression tests were added for MPACT and seven regression tests were added for CTF.

4.1.1 CTF VERIFICATION

As a first step, automated regression tests were added for the power and TH forcing function capability (i.e. time-dependent power and TH boundary condition specification) in CTF, to ensure that this capability was well-tested for transients. A Takahama RIA transient model for standalone CTF, which was created for a previous milestone [4], was added to the automated test suite. This test employed a power forcing function to reproduce the time-dependent power profile from this experiment.

Addition of this test exposed the need for an enhanced test harness for transients which is capable of comparing outputs at numerous points in time during a transient, as opposed to the existing test harness which compares only the results at the final timestep. A new transient test harness was therefore created, which required several steps. The first was the addition of a new 'ChanDiff' class to the CTF python utilities, which have been named 'pyCTF'; this class is used to compare two 'channels.out' files at any number of time points which exist in these files. Then an additional flag was added to the 'test_res' script to allow comparing a 'channels.out' file against a gold file using the 'ChanDiff' class, in addition to (or instead of) comparing the VTK files as was previously done. During this work, the 'Utils' directory in the CTF repository was reorganized in a more logical fashion, including splitting the main directory into 'UnitTest' and 'pyCTF' subdirectories, each containing the appropriate utilities.

In addition to the Takahama RIA regression test, which tested the power forcing function capability, additional regression tests were added to cover the TH boundary condition forcing functions, which allow for time-dependent inlet flow, inlet enthalpy, and outlet pressure boundary conditions. An existing single-channel coverage test, 'cov49', was already implemented to test the pressure forcing function, so additional tests were added based on 'cov49' to test the inlet flow and inlet enthalpy forcing functions. Results for these simple single-phase flow tests were straightforward and precisely matched the expected behavior during and after a linear ramp of the relevant boundary condition.

The testing of the forcing functions will support future transient work such as loss-of-flow accidents. The power (or TH boundary condition) forcing functions are not currently used for coupled RIA analyses, as MPACT sets the power distribution each time it calls CTF during a transient. However, this feature will provide a means for smoothing the transient boundary condition change between calls to CTF_Solve_Transient if it is deemed necessary.

Four single-rod regression tests (each with four CTF channels) were added to the CTF Multistate driver to protect the new transient timestepping and transient coupling features,

and to ensure the defects mentioned in Section 3.2 were fixed correctly. The cases are as follows:

- 'singlerod_transient': performs a 2-second null transient with 0.1 second time intervals requested from $t=0s$ to 1s, and 0.2 second time intervals from $t=1s$ to 2s. This case was run with standalone CTF and through the multistate driver to demonstrate simulation results are identical for the two different use cases.
- 'singlerod_transient_ss': performs a steady-state calculation followed by the same transient as in 'singlerod_transient'. This is representative of the behavior performed in coupled MPACT-CTF runs, where MPACT will first run CTF to steady state before starting the transient.
- 'singlerod_transient_ss_changing_TH': same as 'singlerod_transient_ss', except that the TH boundary condition 'setter' functions for inlet flow, inlet temperature, and outlet pressure are called at various points in the transient.
- 'singlerod_transient_ss_small_dt': reduces the requested time intervals by a factor of 100, such that the CFL-limited CTF timestep size exceeds the requested time interval (This tests the defect fix described above).

The work described in this subsection was performed under PHI Kanban Tickets #4410, #4628, #4640, and #4748.

4.1.2 MPACT VERIFICATION

For the MPACT verification, the previously developed regression test, `MPACT_exe_testValid_transient_4-mini_3D` was modified to run with CTF for the T/H feedback rather than the simplified internal T/H. This was added as a new regression test called `MPACT_exe_testValid_transient_4-mini_3D_CTF`.

The 4-mini test case consists of a 3x3 block of nine fuel assemblies. Each fuel assembly contains a 7x7 grid of pins with a pitch of 1.26 cm. The center pin location consists of an instrument tube, and four other guide tube locations house control rods and inserts. The fuel rods consist of UO_2 pellets with a radius of 0.4096 cm and height of 209.16 cm, helium fill gas, and 0.057 cm thick Zirc4 cladding with an outer radius of 0.475 cm. Each assembly has a uniform enrichment: 2.11% in the center and corner assemblies and 2.619% in the central side assemblies. The center assembly contains a control rod bank consisting of four B_4C control rods with AIC tips. The central side assemblies contain four borated Pyrex inserts in the empty locations, and the corner assemblies contain four stainless steel inserts in the empty locations.

The moderator is water containing 1300 ppm boron with an inlet temperature of 565 K and flow rate of 131 kg/s. The active fuel region of the core contains three grid plates. The initial core power is 100% of rated, and the control rod bank in the central assembly is fully inserted at $t=0$. The "4-Mini Test Problem is shown in Figure 10.

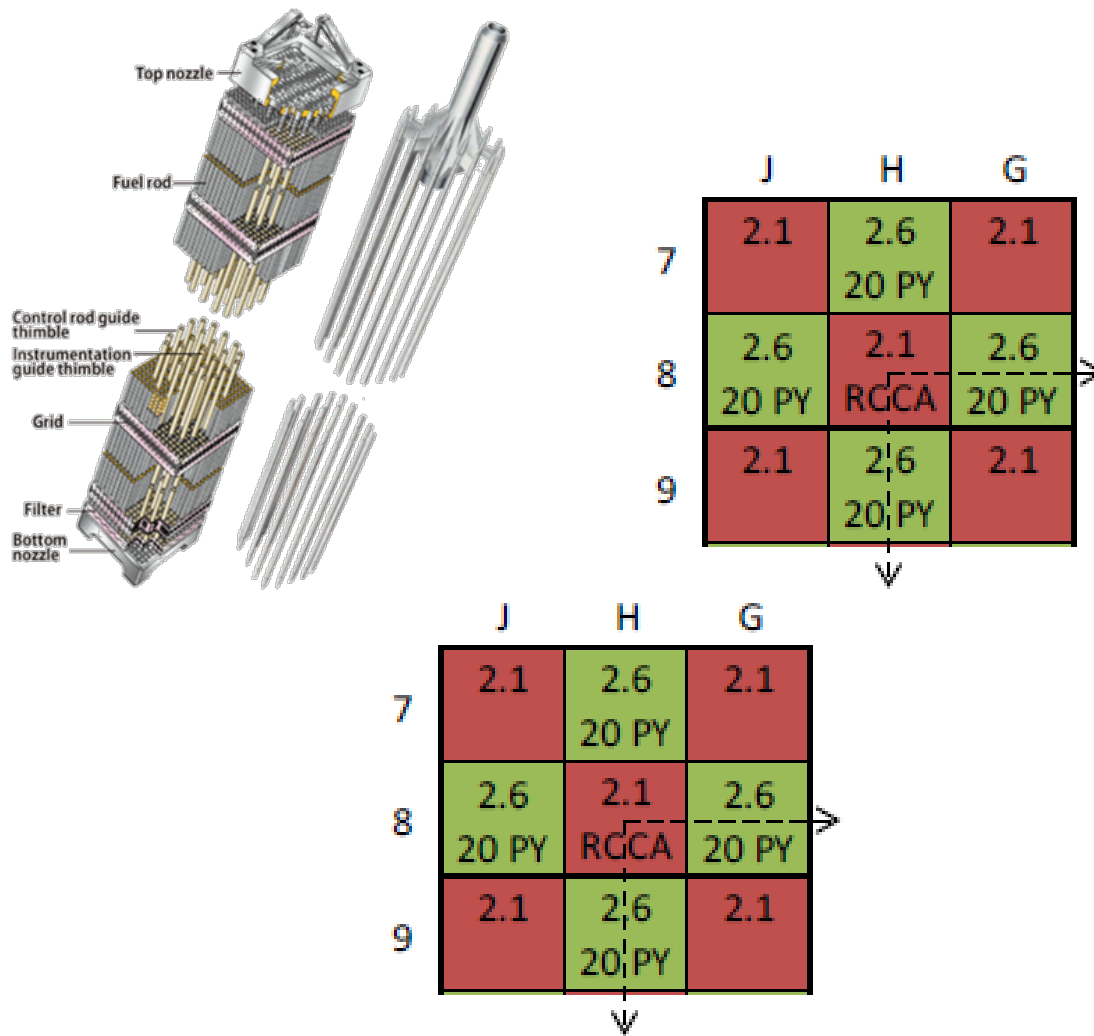


Figure 10. “4-mini” Transient Test Problem

The miniature core is represented in VERA-CS with quarter core symmetry and reflective boundary conditions. The gap, plug, and plenum regions below and above the active core are included in the neutronic model with vacuum boundary conditions beyond to accurately capture the axial leakage.

For the neutronics solution, the MPACT solver used Chebyshev-Yamamoto quadrature (4 azimuthal angles and 1 polar angle per octant) and 0.08 cm ray spacing. For the scattering source, the transport-corrected P0 method was utilized. The 8 group mpact8g_70s_v4.0m0_02232015.fmt cross-section library was used. The axial solution was obtained with multigroup NEM, and multigroup CMFD was utilized for acceleration. The model uses very coarse discretization and the 8-group cross section library for testing. This is to enable the test to run with minimal resources.

For the T/H solution, CTF only considers the active fuel portion of the core, which is divided into 28 axial nodes. The axial levels are defined to explicitly include the spacer grids with uniform spacing between the grids. Only radial conduction is considered with ten radial rings for heat conduction.

The transient is initiated by withdrawing the control rod bank 36.3 cm over 25 ms, which corresponds to a reactivity insertion of $\beta_{1.05}$. The transient is then allowed to run for a total

of 0.1 s. Time steps of 5 ms are utilized. The Transient Multi-level method was employed in MPACT [5].

A rod ejection is simulated for 5 time steps, followed by an additional 15 time steps. The output of the original test is compared with the new test in Figure 11 and Figure 12. The results for using CTF and using simplified TH are similar. The following section on the HZP case describes the reason for these differences, which apply to this case as well. Note that the peak amplitude and peak time for the simplified TH case (roughly 3500% power and 0.055 seconds) differs from the values reported in a previous CASL report (roughly 5500% power and 0.45 seconds); this was due primarily to using an inlet coolant temperature of 565 K, as opposed to 600 K as was used in the previous report. The inlet temperature was reduced in the present study (both for the CTF and simplified TH cases) for simplicity, to avoid reaching CHF conditions in the CTF model. The simplified TH model does not include a CHF correlation, but its inlet temperature was reduced to 565 K as well for consistency of comparison.

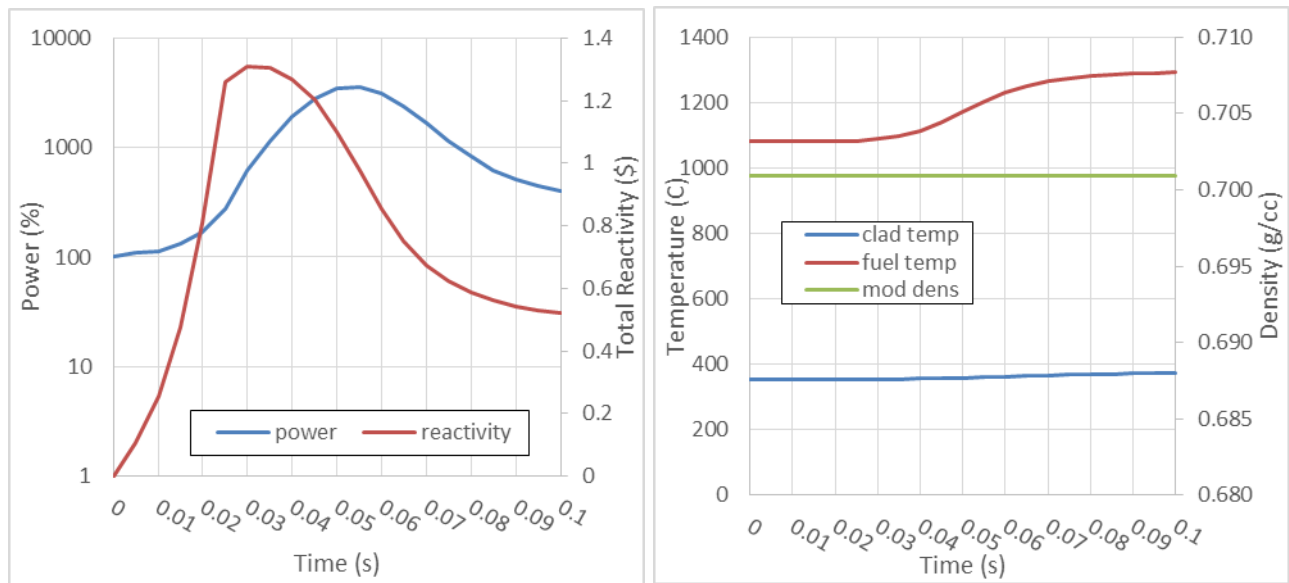


Figure 11. Results for transient 4-mini 3D regression test with simplified T/H

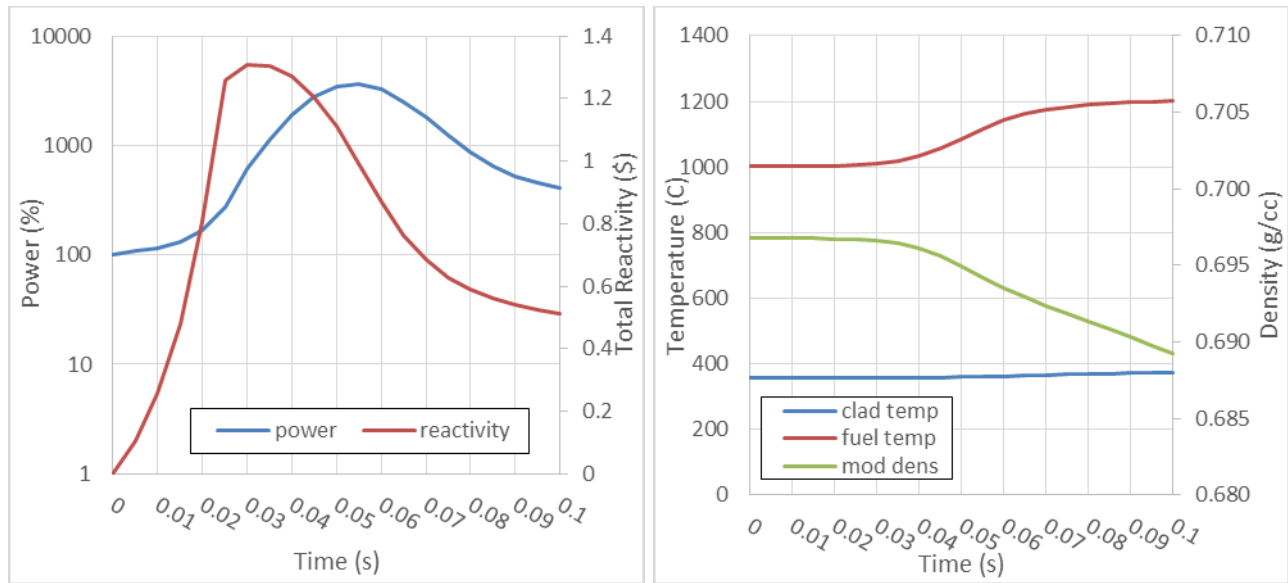


Figure 12. Results for transient 4-mini 3D with CTF

In addition to this test a null transient regression test was also developed, to primarily ensure that the code will execute without issues.

An additional model was run to examine the coupled code performance when starting from 1% power; this will be referred to as HZP in this document. For comparison, this modified transient was run with both the existing simplified T/H in MPACT and coupled to CTF. An inlet temperature of 550 K and a timestep size of 0.0025 s was used for both cases.

The total core power for the transients is shown in Figure 13. The peak power for the coupled transient is about 9% higher than the simplified model. The simplified T/H model employs an adiabatic approximation for the course of the transient. In execution, this amounts to solving the radial heat conduction in the fuel rods with a constant-in-time heat flux from the cladding to the moderator as a boundary condition. As the fuel temperature rises, the actual heat flux to the moderator will also rise, allowing more heat to escape the fuel. Therefore, the adiabatic assumption artificially inflates the fuel temperature during the power pulse. This in turn increases Doppler feedback and explains why the simplified T/H produces a lower peak power than the CTF T/H.

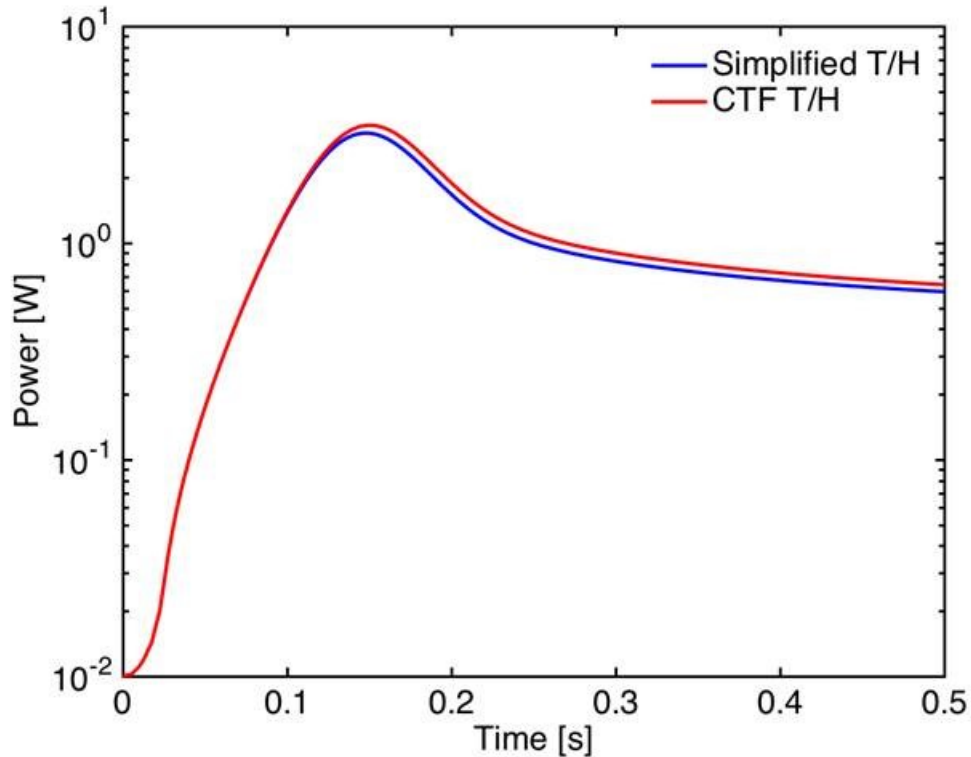


Figure 13. Total core power evolution for 4-mini transient.

To verify this effect, the fuel temperature evolution during the transient was also investigated. Figure 14 shows the core-averaged fuel temperature during the course of the transient. While the temperature evolution appears quite similar for simplified T/H and CTF T/H, inspection of the core-averaged fuel temperature difference between the two methods (also shown in Figure 14) reveals subtle, but notable features. The two methods show excellent agreement for the initial steady-state solve. As the transient progresses, simplified T/H does indeed over-predict the fuel temperature relative to CTF, as expected.

After the power pulse, however, the CTF calculated temperature continues to rise at a faster rate than simplified T/H. Possible explanations include minor differences in the temperature-dependent fuel properties used in each code (the simplified TH model uses a simple power law for thermal properties versus temperature, while the CTF empirical curves are more complex), differences in clad-to-coolant heat transfer in each code, and differences in coolant density in each code (the simplified TH uses a constant coolant density while CTF varies the coolant density with enthalpy).

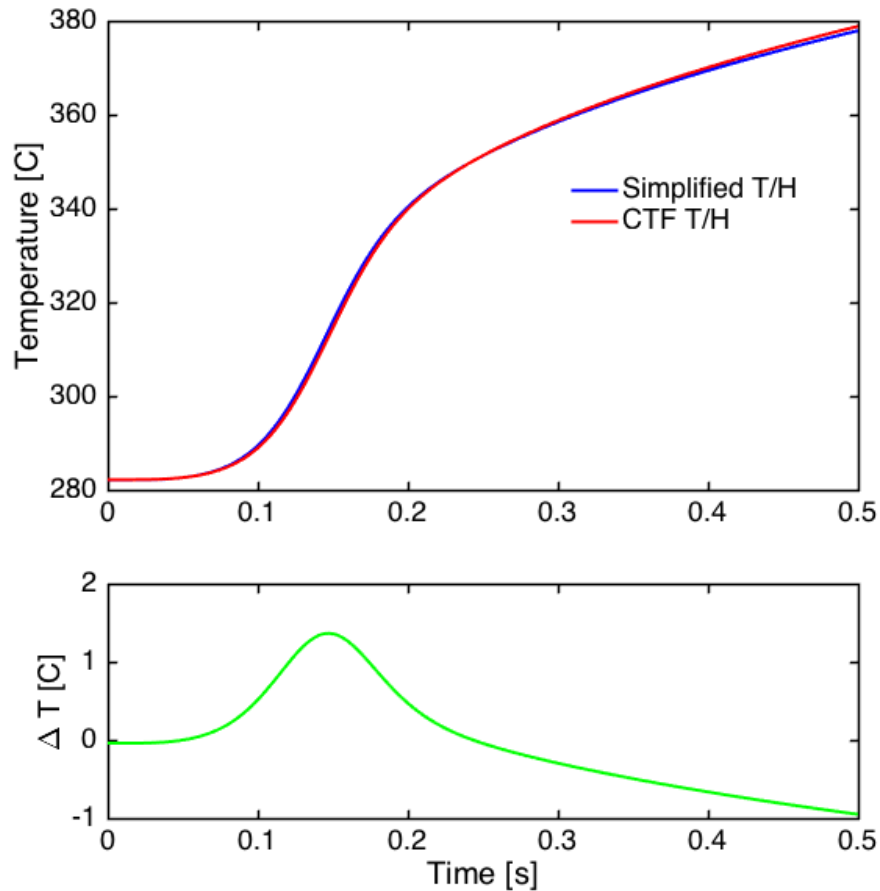


Figure 14. Core-averaged fuel temperature and difference for 4-mini transient.

4.2 DEMONSTRATION PROBLEMS

Two problems were demonstrated with the new CTF coupling capability. In each problem there are substantial components to the problems that make them unrealistic and irrelevant for conventional reactors, but sufficient for demonstration of the expected physical phenomena.

4.2.1 HYPOTHETICAL MINI-CORE REACTOR

The first demonstration problem is a hypothetical mini-core reactor. The core size, rated thermal power, rated flow, and inlet temperature are based on a conceptual mini-core of a standard 4-loop core. The assembly, control rod, and insert design data is taken from Watts Bar Unit 1, cycle 1. A baffle similar to that of WB1 is also present. The core loading pattern and control rod layout in the core are entirely fictitious. The core was also shortened. The loading pattern and control rod bank description are shown in Figure 15.

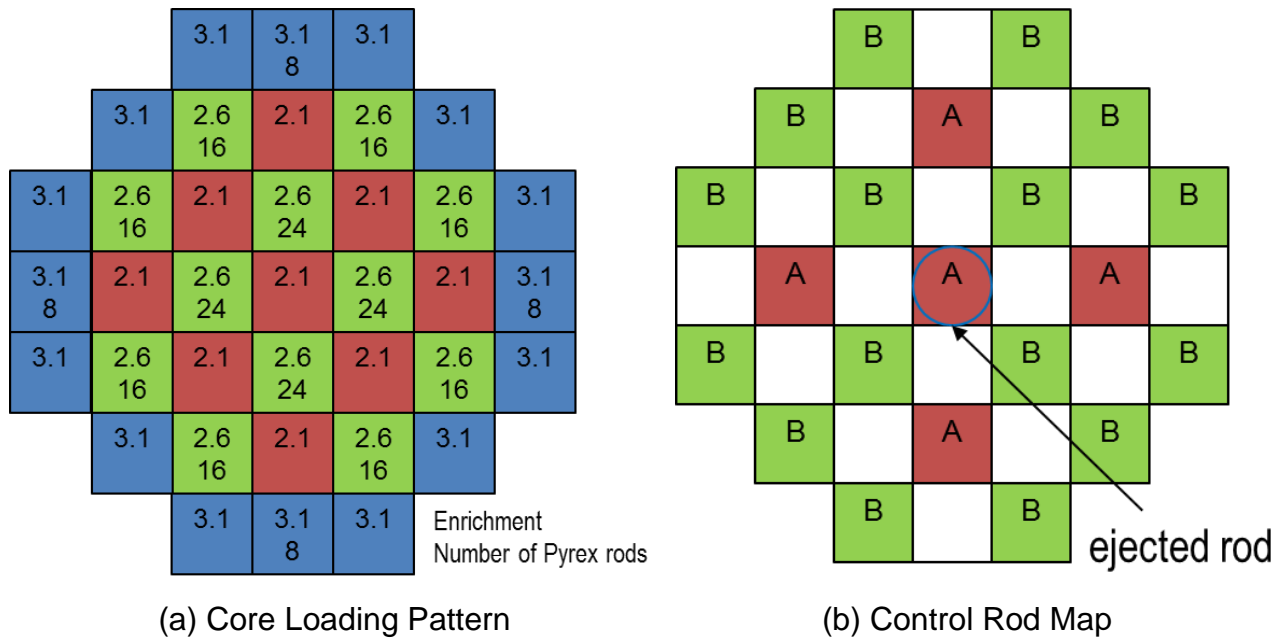


Figure 15. Hypothetical Mini-Core Loading Pattern and Control Rod Map

For the rod ejection accident, the cycle is first simulated to end of cycle, a core average exposure of 12 GWd/MTU. The initial condition of the transient is hot full power. The central rod is assumed to be ejected at time zero and be fully ejected at 0.08 s at constant velocity. This corresponds to the speed of a rod eject at constant velocity from a typical 4-loop PWR. At the initial condition the delayed neutron fraction, β , is calculated to be 0.00565, and the static rod worth of the ejected rod is \$2.42. This is about twice as high as reactivity insertions normally analyzed for super-prompt reactivity insertion accidents.

Additionally, the reactor SCRAM signal is assumed to trip when the core power level reaches 110%. This corresponds to 0.012 seconds into the transient. A 0.4 second delay is assumed for when the scrammed rods start moving. The transient was then simulated out to 0.6 s. This gives a total of 150 time steps, plus the initial steady-state solve.

For computational model, default discretizations were used for the MOC transport and spatial mesh. This means 0.05 cm ray spacing, 16 azimuthal angles, 2 polar angles, 3 rings in the fuel and one in the moderator and 8 azimuthal sectors in a pin cell. The default cross section library, `mpact51g_71_v4.2m5_12062016_sph.fmt`, was used. The default values for CTF were also used. A constant 4 ms time step was used for the MOC with an implicit Euler time stepping scheme with TML acceleration.

The problem was decomposed in space into 704 domains, making each domain the size of a 2-D lattice. The simulation was performed using Titan [6] and took approximately 10 hours. Titan is known to be about half as fast as other clusters used by CASL. Two simulations were performed: one with simplified T/H and one with CTF for the feedback. The former taking approximately 9 hours of wall time and the case with CTF taking approximately 10.5 hours.

In the results below we compare the simplified T/H, which has no transient heat convection and uses an adiabatic approximation for the fuel to the CTF result. First we examine the total reactivity and power during the transient. These are shown in Figure 16.

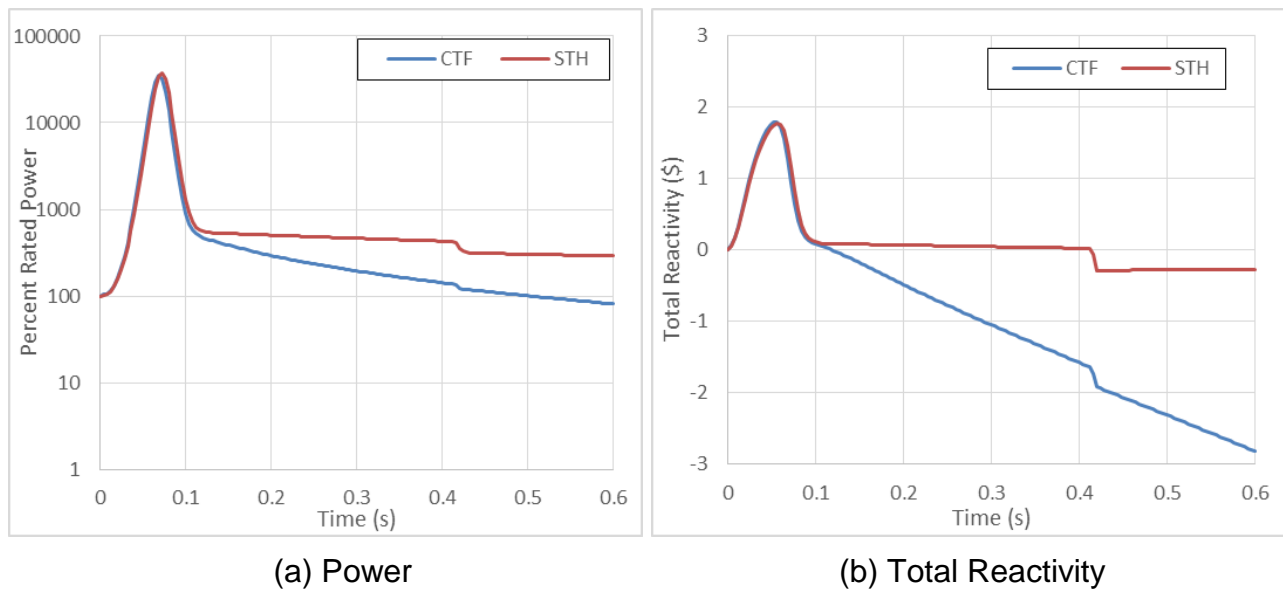
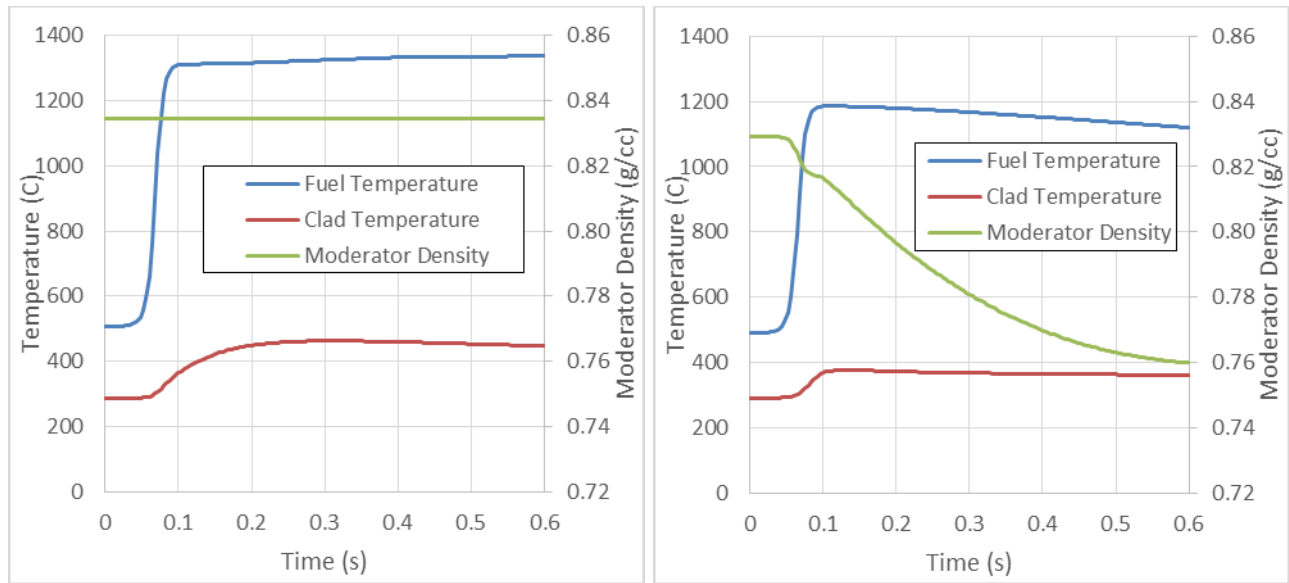


Figure 16. Neutronic results for Mini-Core REA accident with SCRAM

In Figure 16 we observe that both forms of feedback agree well between 0 and 0.1 seconds, about the full width of the pulse. This is expected since the primary form of feedback in a superprompt RIA is Doppler. The SCRAM at 0.412 seconds is also visible in these plots. The worth of the SCRAM is not that much however because the initial reactivity insertion and power pulse is so high, and so fast. There is also a clear difference in the asymptotic behavior between the two feedback methods. This is also expected since CTF is modeling the transient convection and the simplified T/H is not. The downward slope of the reactivity in Figure 16(b) is the result of the change in moderator density as indicated in Figure 17. Another feature of note in Figure 16 is the time at which the convection appears to have an effect. This is typically thought to occur closer to 0.2 or 0.3 seconds, but is observable here around 0.1 seconds. This is explained by the extremely high peak power caused by the large reactivity insertion, and also in part by the models used in the conduction, which correspond to steady state behavior and still need to be updated for the transient conditions of this simulation.

Next we show the pellet average fuel temperature, clad temperature, and moderator density. In Figure 17 it is observed that the simplified T/H solution is not convecting heat. This is indicated by the constant moderator density. This results in the fuel and clad temperature continuing to rise after the pulse. In contrast for CTF, the convection becomes apparent shortly after the pulse and this causes the fuel and clad temperatures to decrease after the pulse. This suggests the underlying physics are represented in the simulation. Absent from Figure 17, is any evidence of the SCRAM at 0.412 seconds.



(a) Simplified T/H

(b) CTF

Figure 17. TH results for Mini-Core REA accident with SCRAM

4.2.2 WATTS BAR

For the Watts Bar demonstration problem, we revisit one of the demonstrations from FY16 DOE reportable transient milestone report [7], specifically case 2 which is an ejection of the central rod. The static rod worth for the central rod is a little less than \$0.25. The previous demonstration was simulated from HFP at BOL, here we simulate at HZP.

This simulation also used default discretizations in VERA and was run on 4234 cores on Titan using spatial decomposition. The model employed quarter symmetry and required between 2 and 4 GB of memory per core. The runtime was approximately 4 hours.

Results are shown in Figure 22 through Figure 21. This case represents a very mild transient in which an initial power increase of roughly 1.2 times the initial power occurs due to the increase in prompt neutron production related to the reactivity insertion, followed by a gradual increase in power due to delayed neutron buildup. This buildup occurs at a longer timescale than shown in the plot; however, the solution was stopped at 0.3 seconds to capture the initial power increase only.

The intention of this case was to perform a simple, mild transient with the quarter-core Watts Bar model. Future work will examine the behavior of this model for a HZP superprompt-ejection case, as well as a HFP ejection case, to provide a more relevant demonstration.

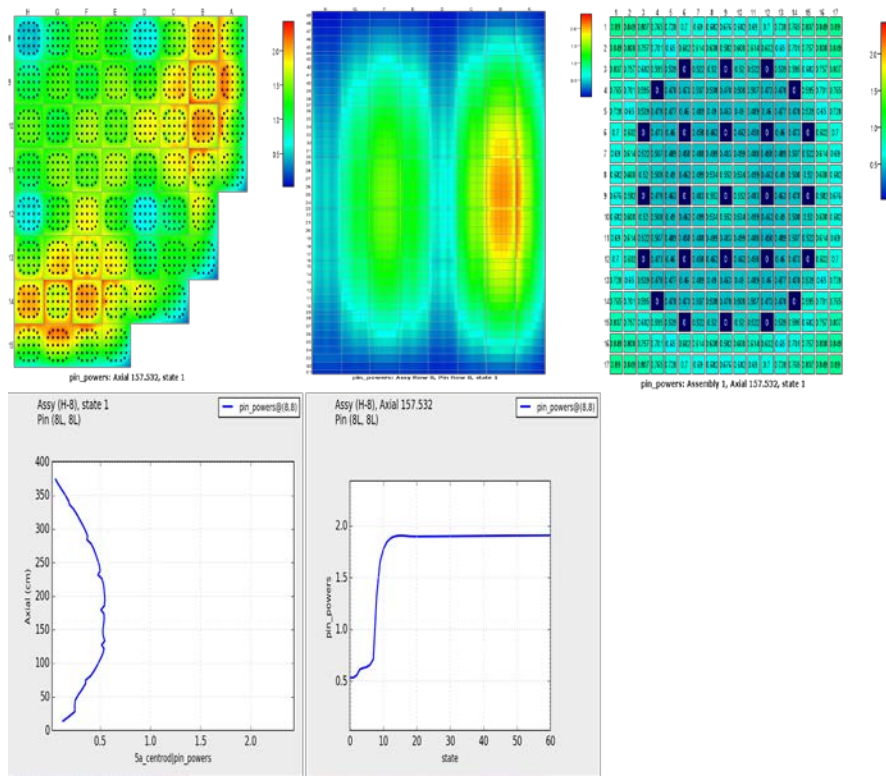


Figure 18. Watts Bar HZP 0.25\$ ejection case, $t=0.005$ s

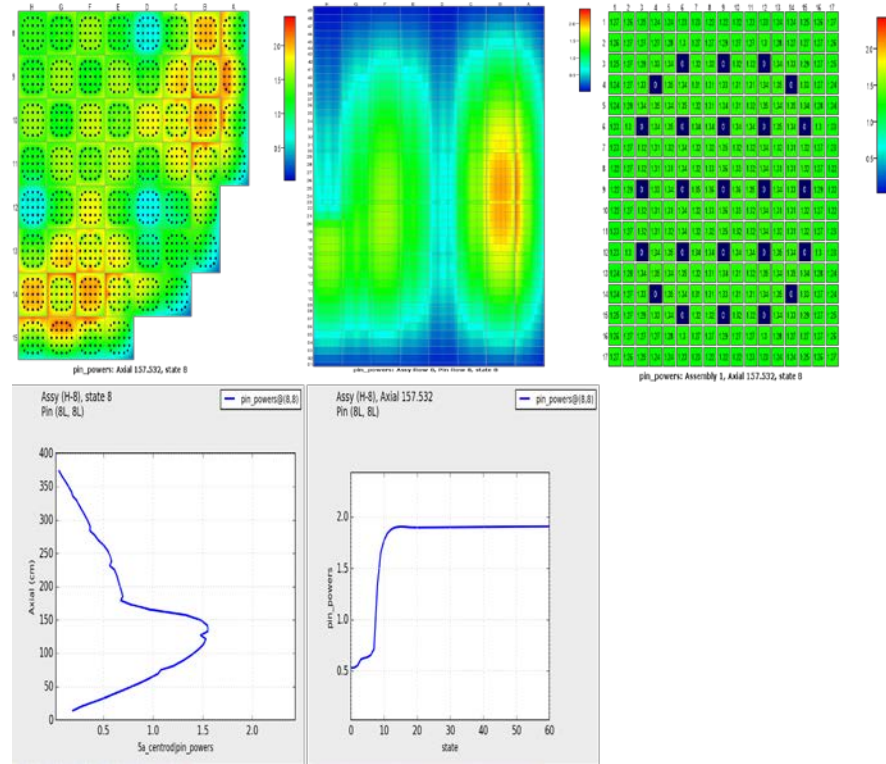


Figure 19. Watts Bar HZP 0.25\$ ejection case, $t=0.04$ s

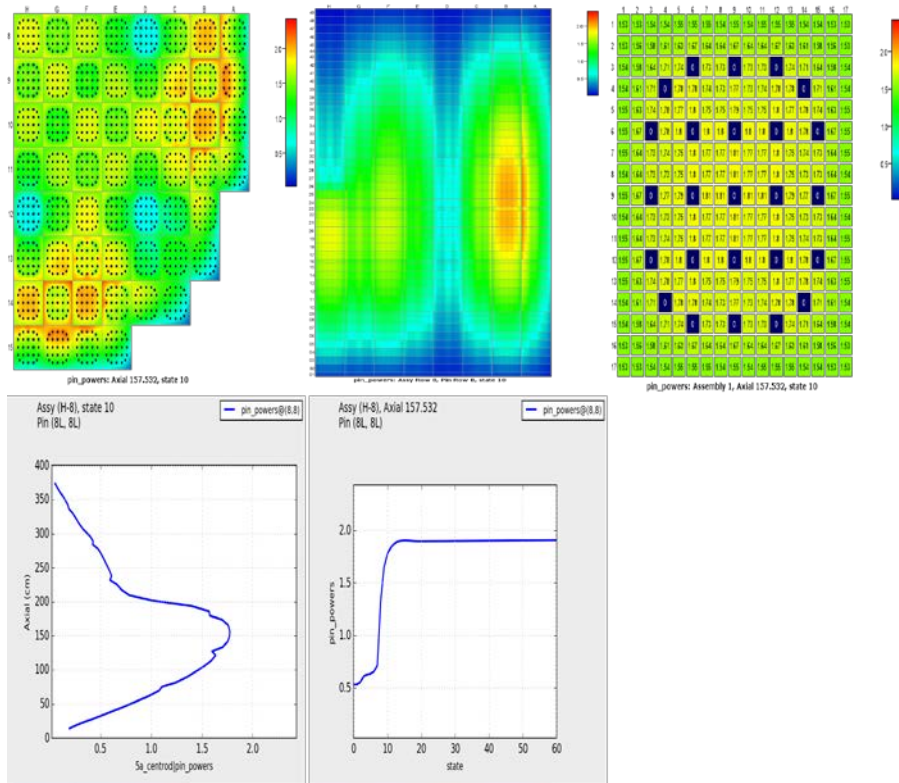


Figure 20. Watts Bar HZP 0.25\$ ejection case, t=0.05 s

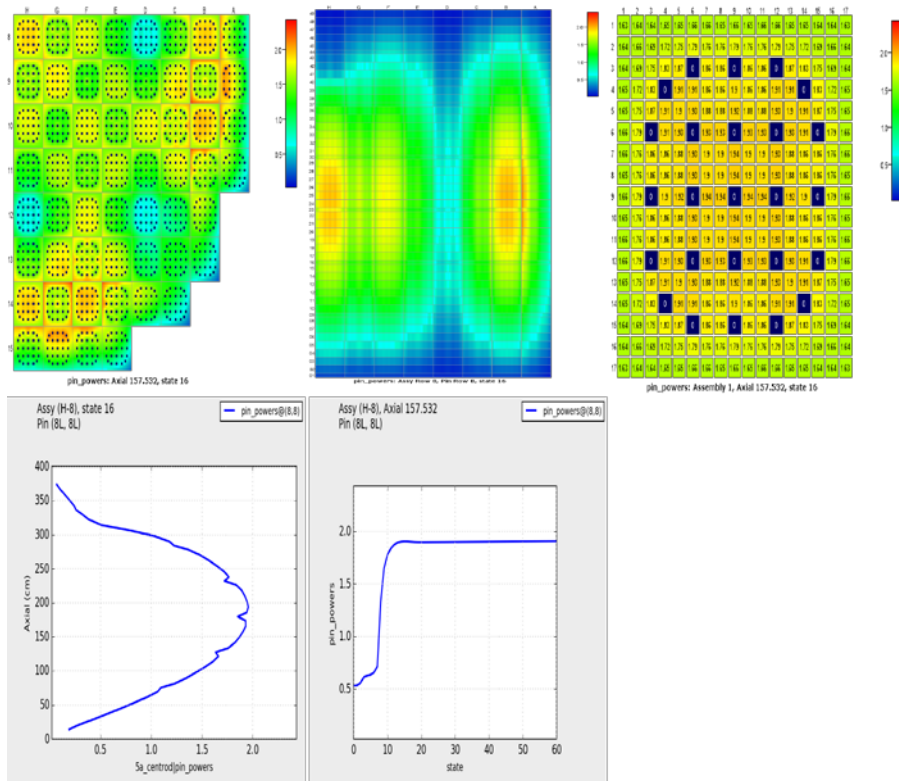


Figure 21. Watts Bar HZP 0.25\$ ejection case, t=0.08 s

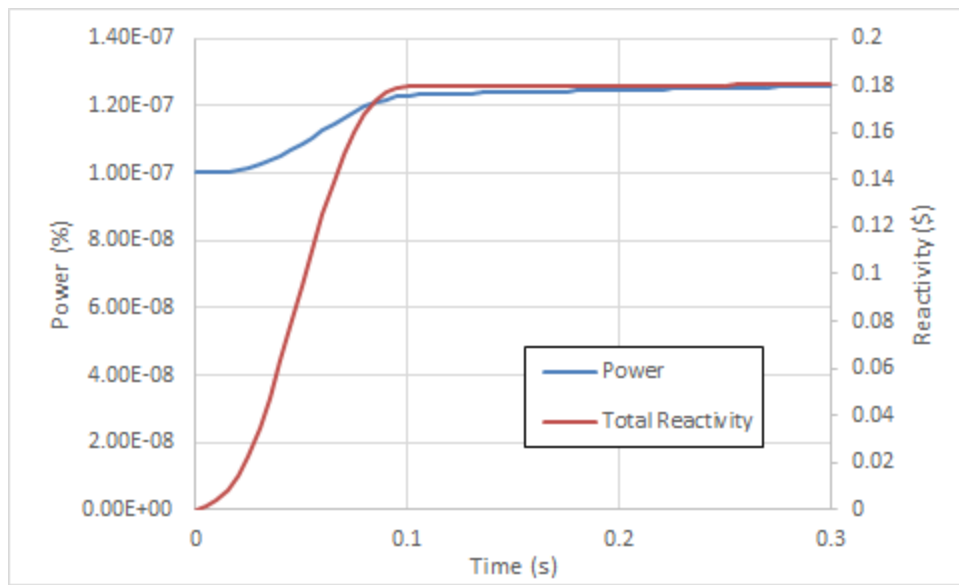


Figure 22. Watts Bar HZP 0.25\$ ejection case: power and reactivity versus time

5 CONCLUSIONS AND FUTURE WORK

This milestone has demonstrated a basic capability to model postulated rod ejection events with a 3D coupled neutronic-T/H model in VERA-CS. The code behaved qualitatively as expected during the RIA transients, with an initial power spike followed by a power decrease due to fuel heat-up and Doppler feedback, and a subsequent power level determined by delayed neutrons. Unlike MPACT's simplified TH model, CTF was able to account for realistic clad-to-coolant heat transfer and its effect on fuel temperatures and coolant density at longer simulation times after the power spike.

Future efforts will focus on methods improvements, code output improvements, and additional validation and demonstration work, as described below.

5.1 METHODS IMPROVEMENTS

The preliminary results shown in this report utilize a constant gap conductance and temperature-dependent (but not burnup-dependent) fuel and cladding properties. CTF contains the following optional models which are being evaluated and, if needed, improved to properly capture the dynamic fuel behavior during a RIA event:

- Fuel and cladding deformation model: pellet cracking, fuel sintering, fuel relocation, fuel and cladding thermal expansion, cladding elastic deformation, dynamic gap closure
- Dynamic gap conductance model: gap thickness dependence, gap gas pressure, gas conductivity, radiative heat transfer, pellet-clad contact resistance

Current testing has involved comparing CTF predicted fuel temperature behavior against the Halden experiments as well as FRAPCON and BISON for steady state simulations [8]. This has revealed CTF model improvement needs, including burnup-dependent pellet swelling, fuel relocation, densification, and clad creep. Further work will also include transient fuel model testing and code-to-code verification. In late FY17, efforts will include enabling the CTF dynamic gap conductance model through the VERAIn file, allowing it to be used for coupled simulation. By FY18, the goal is to have a working MPACT-CTF-BISON capability relying on 1.5D BISON. The CTF dynamic fuel models would be at least an interim solution for fuel modeling until the BISON coupling is ready. However, if 1.5D BISON coupling is deemed too computationally expensive for pin-resolved core modeling applications, the CTF dynamic fuel models may be selected as a viable option while giving improved runtimes. In this case, the 1.5D BISON capability would be used to inform the CTF dynamic fuel modeling and used for code comparison purposes.

An additional primary area of further development for the VERA-CS RIA transient capability is the investigation of transient boiling and CHF models. This work will leverage the available experimental data and knowledge of boiling effects in rapid heating scenarios. For example, experimental data from the PATRICIA facility [9] suggests CHF values during rapid wall heating that are roughly 50% higher than corresponding steady-state CHF values. This was attributed to near-wall coolant effects (thermal boundary layer effects, bubble formation time, and the propagation of hydrodynamic instabilities) which lead to the inadequacy of steady-state relationships in predicting boiling behavior under rapid-heating conditions. Additional boiling and CHF models will be implemented within CTF in the FY18 timeframe in an effort to more accurately predict the dynamic fluid thermal behavior for RIA applications.

Future efforts will examine improved CMFD solver improvements (improved matrix preconditioning) for the MPACT neutronic solution during transients. Additionally, an adaptive timestepping algorithm for the Transient Multi-Level Solver in MPACT will be examined, to dynamically adjust timestep sizes on-the-fly. This will lead to a more robust, stable neutronic solution while also reducing runtime.

5.2 CODE OUTPUT IMPROVEMENTS

The ability of MPACT to output individual component reactivities (control rod reactivity, Doppler reactivity, moderator density reactivity, etc.) will be examined for future implementation, to allow greater insight into the physics and VERA-CS predictive capabilities for transients.

Future work will also include a mechanism for applying conservatism to the MPACT-CTF calculation, which will be useful for industry partners in the licensing space.

5.3 ADDITIONAL VALIDATION AND DEMONSTRATION ACTIVITIES

Standalone CTF RIA validation for the NSRR fuel rod tests was completed in 2014. MPACT validation using the built-in simplified TH model was performed for the SPERT experiments in 2016.

Future VERA-CS transient validation activities will focus primarily on development of a coupled MPACT-CTF model for the SPERT small reactor RIA tests. These tests, which include both superprompt- and subprompt-critical reactivity excursions, will provide an integral validation exercise for neutronics, fuel heating, and clad-to-coolant heat transfer.

Further analyses on the Watts Bar quarter-core model will be performed. An FY18 L1 milestone will focus on PWR control rod ejection accident simulation using VERA-CS, to demonstrate the full coupled transient capability for PWRs under realistic conditions.

6 REFERENCES

- [1] NRC memorandum, *Technical and Regulatory Basis for the Reactivity-Initiated Accident*, ADAMS ML ML070220400, 2007.
- [2] NRC, "Pressurized Water Reactor Control Rod Ejection and Boiling Water Reactor Control Rod Drop Accidents," DG-1327, 2016.
- [3] B. Kochunas et al., "VERA Core Simulator Methodology for Pressurized Water Reactor Depletion," *Nucl. Sci. and Eng.*, vol. Accepted for Publication, Jan. 2017.
- [4] Y. Sung, J. Yan, L. Cao, V. Kucukboyaci, E. Tatli, M. Christon, J. Bakosi, R. Salko and H. Zhang, "Assessment of Multi-Scale Thermal-Hydraulic Codes and Models for DNB Challenge Problem Applications," CASL Report L3.AMA.CP.P8.01, 2014.
- [5] CASL-U-2016-1188-000.
- [6] "Titan User Guide," Oak Ridge Leadership Computing Facility, [Online]. Available: <https://www.olcf.ornl.gov/support/system-user-guides/titan-user-guide/>. [Accessed 31 March 2017].
- [7] Y. X. A. Z. B. K. D. J. T. Downar, "Transient Capability in MPACT with Internal Heat Conduction Feedback for Analysis of PWR Reactivity Insertion Accidents (RIA)," CASL Technical Report, CASL-U-2016-1188-000, Sept. 2016.
- [8] A. Toptan, R. K. Salko and M. N. Avramova, "Review of CTF's Fuel Rod Modeling Using FRAPCON-4.0's Centerline Temperature Predictions," in *Trans. of the Amer. Nucl. Soc.*, San Francisco, 2017.
- [9] V. Bessiron, "Modelling of Clad-to-Coolant Heat Transfer for RIA Applications," *Nucl. Sc. and Tech.*, vol. 44, no. 2, pp. 211-221, 2007.